Geophys. J. Int. (2003) **152,** 740–748

A direct method of estimating depth to a reflector from seismic wide-angle reflection times

Prakash Kumar, Kalachand Sain and H. C. Tewari

National Geophysical Research Institute, Uppal Road, Hyderabad 500 007, *India. E-mail: prakashngri@rediffmail.com*

Accepted 2002 October 7. Received 2002 October 7; in original form 2001 September 27

SUMMARY

The analysis of wide-angle recordings in controlled source seismics has been an important tool for imaging deep features of the lithosphere. Here we present a simple method of directly calculating the depth to a reflector from wide-angle reflection data without knowing any velocity information or the interface structure of the overlying layers. The method has also been extended to evaluate the average velocity above the reflector. Both theoretical and field examples demonstrate the efficiency of the method.

Key words: average velocity, depth, wide-angle reflection.

1 INTRODUCTION

The wide-angle reflections from various subsurface boundaries within the earth, are generally identifiable in the post-critical range, even with small impedance contrast (Richards 1961; Winterstein & Hanten 1985). Examples may be found in Giese (1976) who presented a review of wide-angle experiments in Central Europe. However, to date, no method exists to directly calculate the depth to a reflector (e.g. Mohorovicic discontinuity) from wide-angle reflection (P_mP) traveltime data. The most commonly used method in order to calculate the interval velocity and thickness of a layer needs an accurate estimate of the root mean square (rms) velocity and the zero-offset two-way (ZOT) time (Dix 1955). Applying Dix's hyperbolic formula to the non-hyperbolic wide-angle reflection times causes large errors in the rms velocity and ZOT time (Sain & Kaila 1994a) and hence in calculating layer parameters.

A number of 1-D methods (Stoffa *et al.* 1981; Schultz 1982; Gonzalez-Serrano & Claerbout 1984; Sain & Kaila 1994b), all assuming a laterally homogeneous velocity structure, exist to calculate interval velocities from large-offset/wide-angle reflection times. The advantages and disadvantages of these methods have been described by Sain & Kaila (1996), who proposed a method of directly calculating interval velocities and layer thickness from a series of wide-angle reflection times from various subsurface interfaces. Since all of these methods are based on the layer stripping technique, errors in the overlying layers would cause errors in the underlying layers. Recently, de Franco (2001) has proposed a method of estimating the interval velocity and thickness of a layer in a horizontally stratified medium from wide-angle reflection data, but it requires the same ray parameter at the top and bottom of the layer concerned. For field data, determination of the same ray parameter at the top and bottom of the layer may be difficult.

Here we present a method that can estimate the depth to a reflector directly from large-offset/wide-angle reflection data without any knowledge of the overlying velocity and interface structure. This method provides a quick starting model for fast computation of 2-D forward or inverse modelling to further refine the velocity structure. This method also serves as an independent test to validate the existing 2-D models by calculating the average 1-D model.

2 METHODOLOGY

Here we present an approach to estimate the reflector depth in 1-D layered structures without initially estimating the seismic velocity as a separate parameter. The mean average velocity above the reflector can be estimated once the depth has been calculated. The method assumes that the traveltimes for any layer are similar to the single-layer case.

Let us use an n-layered (e.g. four-layer) earth model (Fig. 1a), in which the ray leaves the source, S at the surface, traverses through the layers following Snell's law, becomes reflected at O from the base of the nth (fourth) layer, returns through the overlying layers and eventually emerges at the receiver R at a distance X after time T. X and T are related to the layer parameters (velocities and thicknesses) by non-hyperbolic parametric equations (Slotnick 1959) as

$$T(p) = 2\sum_{i=1}^{n} \frac{h_i}{V_i\left(1 - p^2 V_i^2\right)^{1/2}} \tag{1}$$

$$X(p) = 2p\sum \frac{h_i V_i}{\left(1 - p^2 V_i^2\right)^{1/2}} \tag{2}$$

where $p = \sin\theta_i / V_i = \text{constant}$ is the ray parameter, θ_i, V_i and h_i are the angle of emergence, the velocity and the thickness of the ith layer, respectively.

Kaila & Krishna (1979) defined the effective velocity V_{eff} along the ray path SOR as the sum of the straight paths (dashed line) divided by the actual traveltimes T through the curved path for a reflector at depth Z and thus

$$V_{\text{eff}} = (\text{SO} + \text{OR})/T = (X^2 + 4Z^2)^{1/2}/T. \tag{3}$$

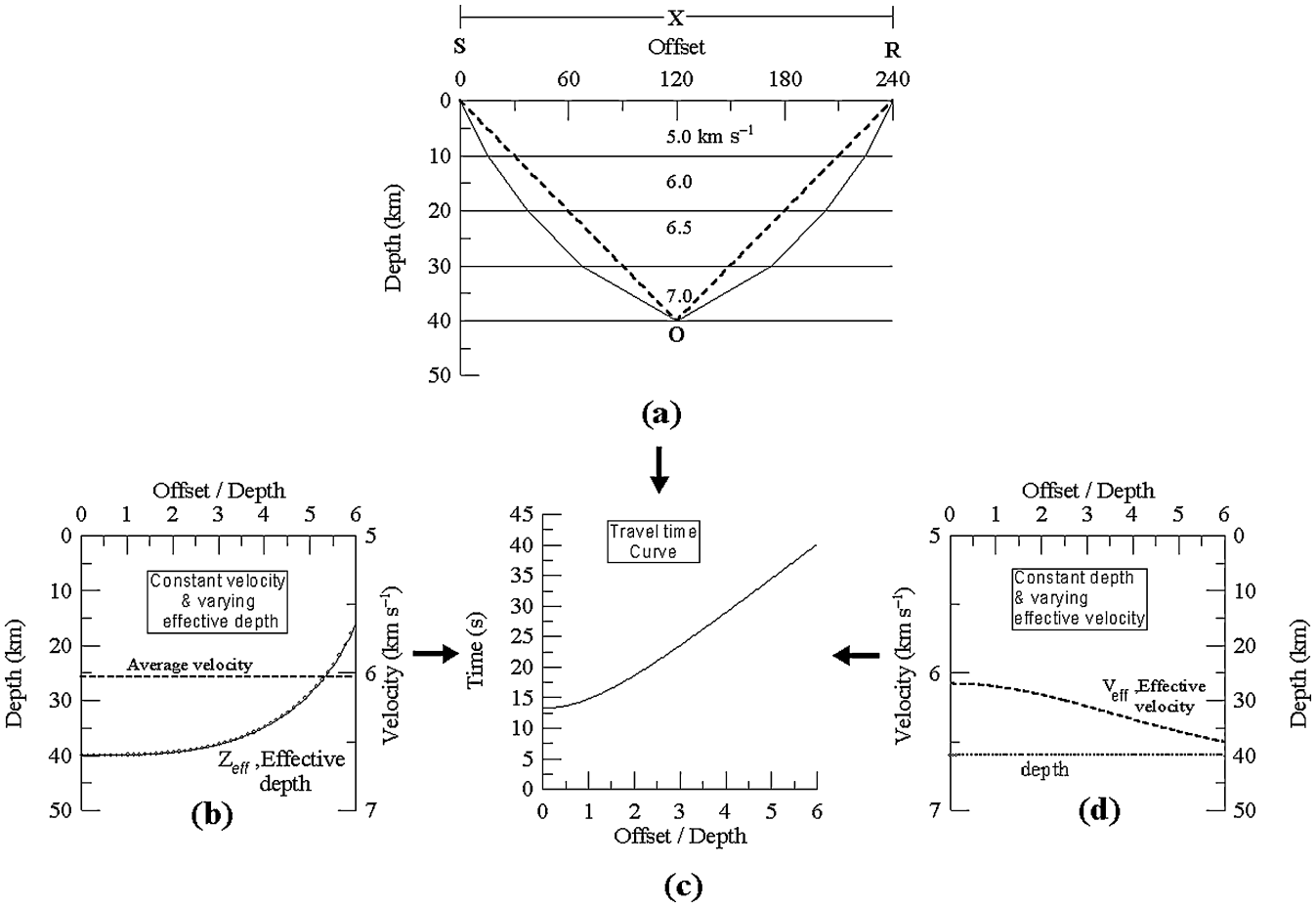

Figure 1. (a) A conceptual model representing a multilayered earth. The solid line (———) is the ray path for a reflection from a horizontal boundary underlying a vertically inhomogeneous medium consisting of isotropic and horizontally homogeneous layers. The broken line (- - - - - -) represents the straight path at the same reflection point if the whole layered model is replaced by a single medium. The traveltimes (Fig. c) generated from the bottom of the model can be matched either to a single layer of constant velocity and varying effective depth shown in (b) or by a constant depth and varying effective velocity field shown in (d). The abscissae of (b)–(d) are plotted as offset/depth.

Fig. 1 shows the concept of an effective medium. The traveltime curve of the reflection (Fig. 1c) from the bottom layer of the multilayered model in Fig. 1(a) can be matched either by a single layer with the same velocity (e.g. the average velocity of the model) and a depth function (Fig. 1b) called the effective depth Z_{eff} or by a single layer with the same depth and a varying velocity function (Fig. 1d) called the effective velocity V_{eff}. Properties of V_{eff} and Z_{eff} are as follows:

$$V_{\text{eff}} > V_{\text{av}} \quad \text{and} \quad Z_{\text{eff}} < Z \quad \text{for} |X| > 0$$

$$V_{\text{eff}} = V_{\text{av}} \quad \text{and} \quad Z_{\text{eff}} = Z \quad \text{for} X = 0.$$

In an attempt to determine the depth to a reflector from large-offset/wide-angle reflection traveltime data, Kaila & Krishna (1979) used a $T^2 - X^2$ fit that produces the rms velocity (Dix 1955) for near zero-offset data and the slant path rms velocity (Robinson 1983; Al-Chalabi 1974) for larger offset data. The slant path rms velocity is always larger than the rms velocity, which in turn is larger than the average velocity (V_{av}). Sain & Kaila (1994a) show that the percentage errors in both rms velocity and ZOT time increase monotonically by a hyperbolic fit to the successively increasing offset traveltime segments. Hence, the method of Kaila & Krishna (1979) will produce an overestimation of the depth and the error increases monotonically with increasing offset. Besides, Kaila & Krishna (1979) did not perform any velocity analysis.

For a single-layer configuration in which the time–distance relation is purely hyperbolic, V_{eff} is nothing but the actual velocity V of the layer. The traveltime equation for a single-layer medium is

$$T^2 V^2 = X^2 + 4Z^2. \tag{4}$$

Bearing in mind deriving an expression for depth Z that is independent of the velocity V, we take the logarithm on both sides of eq. (4) and then differentiate after T, which results in

$$Z = 0.5\sqrt{XT\left(\frac{dX}{dT}\right) - X^2}, \tag{5}$$

where dT/dX is the slope of the time–distance curve, and is defined as

$$\frac{dT}{dX} = \lim_{\Delta X \to 0} \frac{\Delta T}{\Delta X} = \lim_{\Delta X \to 0} \frac{T(X + \Delta X) - T(X)}{\Delta X}.$$

Application of eq. (5) can accurately determine the depth to the reflector for a single-layer configuration. However, application of eq. (5) to non-hyperbolic reflection data sets from a multilayered earth model overestimates the depth to the reflector owing to the varying velocity function V_{eff}. The estimated depth increases with

a subsequent increasing offset and we define the increasing depth as the slant depth, analogous to the slant path rms velocity.

To compute the correct depth for non-hyperbolic data the traveltimes from each reflector of the model, shown in Fig. 1(a), are generated at 200 m spacing up to an offset/depth of 6 using eqs (1) and (2) and slant depths using eq. (5). We then establish an empirical linear relation between the slant depths and the square of offsets. Therefore, when plotting Z versus X^2, the linear regression line yields the correct depth to the reflector at zero offset (Fig. 2a), as non-hyperbolicity and hyperbolicity coincide only near zero-offset ($dV/dX \approx 0$). Once the depth is known the effective velocities at various offsets can be calculated using eq. (3). Here we find that the linear regression of the square of the effective velocity versus the square of the offset yields the average velocity at zero offset (Fig. 2b) above the reflector. The average velocities corresponding to two successive reflectors are then utilized to calculate the interval velocity in the corresponding depth interval. Depths and average velocities calculated by this method are close to the actual values (see the table in Fig. 2) even for very large-offset reflection data up to an offset/depth ratio of 6, which is more than sufficient for recording of crustal wide-angle reflection data.

The depth estimation using the method discussed above and using the conventional normal moveout equation ($T^2 - X^2$) has been compared in Fig. 3 for a four horizontal plane layer case to show the magnitude of the error involved. To know the effect of increasing offset to the estimated depths using both the methods, we have generated reflection traveltime data up to an offset/depth ratio of 6 with 200 m spacing and grouped them in such a way that the first group includes the first to jth data points, the second group contains the second to $(j + 1)$th, and so on until all data are included (here we use $j = 20$). Using the procedure explained in Fig. 2, we calculated the depth to all reflectors taking the successive traveltime segments containing 20 data points. The Z values for each segment are assigned at the mid-point of the each segment. Small discrepancies between the estimated and real values are caused by the assumption of linearity between Z versus X^2 within the shown range of offset by depth ratio (Fig. 3). It is evident that the depths calculated using the conventional normal moveout equation are greater than the real depths and the discrepancy increases significantly with increasing offset. This is a result of the conventional normal moveout equation that takes the slant path rms velocity (which is always higher than the actual rms velocity) in the depth calculation.

Now we extend the method for dipping layers with reversed seismic data coverage. Eq. (5) has been derived from eq. (3), which is valid only for a plane horizontal layer case. In the case of a dipping layer, application of this horizontal layer equation to the reverse coverage data assumes two horizontal layers: one in the updip direction passing through Q (i.e. QQ′), and the other in the downdip direction passing through P′ (i.e. PP′) cutting the reflector plane just below the shot points (Fig. 4). So for the dipping layer case two depth

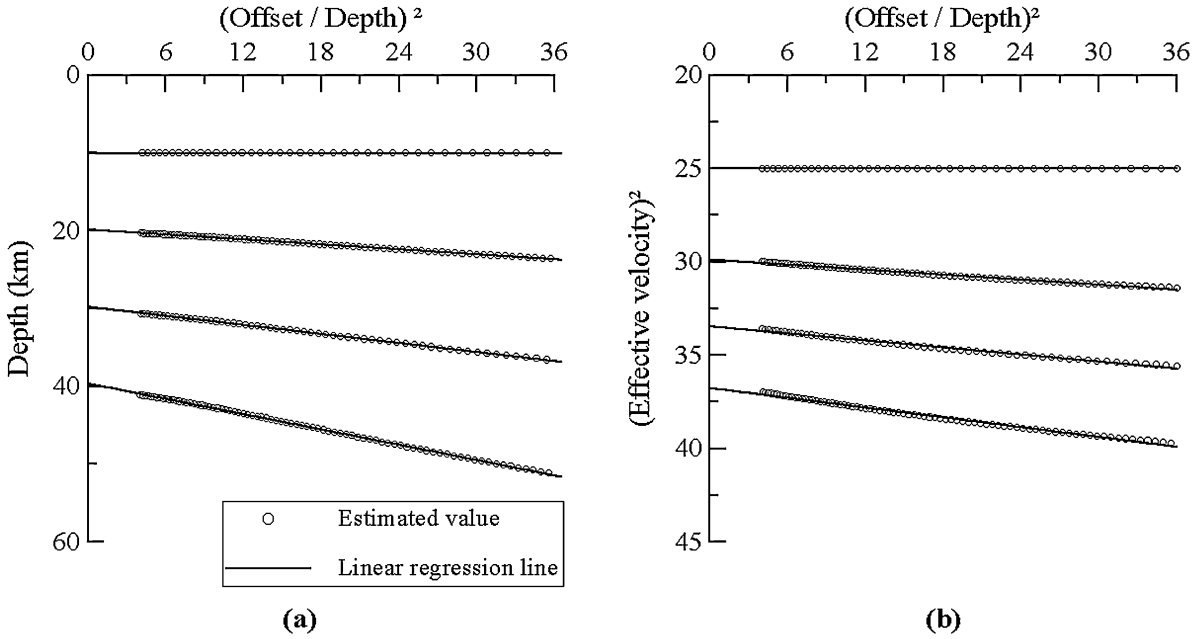

Depth (km)	Interval Velocity (km s^{-1})	Real average velocity (km s^{-1})	Estimated depth (km) Zero-offset depth	Estimated average velocity (km s^{-1}) Zero-offset velocity
10.0	5.0	5.00	10.00	5.00
20.0	6.0	5.44	19.84	5.46
30.0	6.5	5.75	29.77	5.77
40.0	7.0	6.01	39.63	6.06

Figure 2. (a) The estimated slant depths (open circles) obtained using eq. (5) and the zero-offset values are the estimated depths for the corresponding layer. (b) Open circles represent the square of the effective velocity versus the square of the offset. The zero-offset values are the square of the estimated average velocities at the corresponding reflectors. Solid lines denote the regression lines for (a) Z versus X^2 and (b) $V^2_{\rm eff}$ versus X^2, respectively.

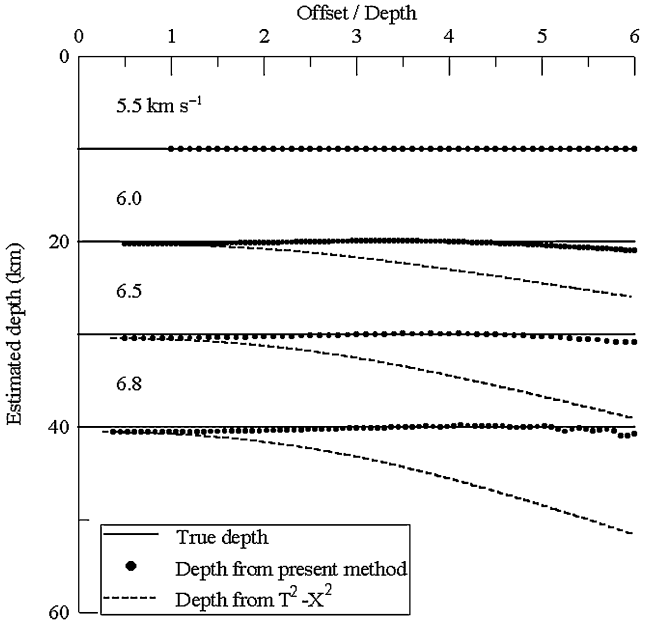

Figure 3. A simplified crustal model showing the reflecting boundaries at 10, 20, 30 and 40 km. The depths to each reflector have been estimated using the present method and the conventional normal moveout ($X^2 - T^2$) equation. The conventional normal moveout equation overestimates the depth with increasing offset.

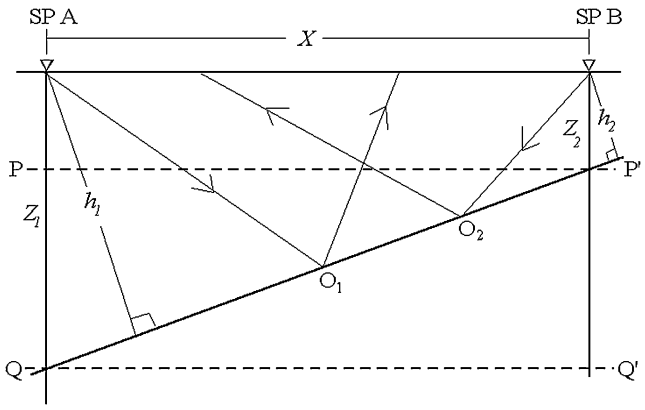

Figure 4. A plane dipping layer case having two shot points SP A and SP B separated by a distance X. Z_1 and Z_2 are the vertical depths, while h_1 and h_2 are the normal depths to the reflector QP′. Application of horizontal layer eq. (5) for this dipping layer case is equivalent to two horizontal layers, one passing through Q (i.e. QQ′) for updip shooting and the other passing through P′ (i.e. PP′) for down-dip shooting.

values (Z_1 for shot point SP A and Z_2 for shot point SP B) are obtained that lie just below the shot point. Synthetic traveltimes at 200 m spacing are calculated from each reflector of the velocity model (Fig. 5a) up to an offset/depth ratio of 6 for both forward and reverse shot points (SP A and SP B). Using the procedures described in Figs 2(a) and (b) we generate plots of Z versus X^2 as shown in Fig. 5(b) and V_{eff}^2 versus X^2 as shown in Fig. 5(c). The zero-offset values of the linear fit in Figs 5(b) and (c) are the respective depths and square of average velocities of various reflectors in the model (Fig. 5a). Here we obtain two interval velocities for two shot points and the arithmetic mean of these two velocities is the estimated interval velocity of the respective layer (Fig. 5a). The estimated depths and interval velocities match quite well with the actual values. It is to be mentioned here that the depth to the dipping reflector can be calculated by this method up to a dip angle of $\leq 10^\circ$. Beyond this dip angle, the approximate linearity between the X^2 versus Z no longer holds well. While studying a number of velocity models with dipping ($>10^\circ$) layers, it has been observed that the present method works for traveltime data with an offset/depth ratio of greater than 2.

The method works very well for the synthetic data. However, for field data that contain noise it may suffer from the following limitations. (1) dT/dX is very sensitive to the spatial sampling of the data, (2) the term within the square root of eq. (5) must always be positive and (3) field data are not exactly 1-D. To overcome the limitations, we smooth the field data by fitting a low-order polynomial of the form

$$T^2 = C_0 + C_2X^2 - C_4X^4. \tag{6}$$

One should not go for higher-order polynomials, as the higher-order polynomials tend to oscillate widely between the observed values and will not mimic the exact traveltime nature of the 1-D model.

Eq. (6) yields,

$$\frac{dT}{dX} = \frac{C_2X - 2C_4X^3}{T}; \quad T \neq 0. \tag{7}$$

Putting eq. (7) in eq. (5)

$$\begin{aligned} XT\left(\frac{dX}{dT}\right) - X^2 &= XT\frac{T}{C_2X - 2C_4X^3} - X^2 \\ &= \frac{C_0 + C_2X^2 - C_4X^4}{C_2 - 2C_4X^2} - X^2; \\ &\geq \frac{X^2(C_2 - 2C_4X^2)}{C_2 - 2C_4X^2} - X^2; \quad \text{if } C_0 \geq 0 \\ &\geq 0; \quad \text{if } C_4 \geq 0 \text{ and } C_2 \geq 2C_4X^2 \end{aligned}$$

and therefore the term within the square root of eq. (5) must be positive.

3 SYNTHETIC AND FIELD EXAMPLES

A crustal-scale 1-D velocity model consisting of four layers, each 10 km thick and with velocities of 5.0, 6.0, 6.6 and 6.8 km s^{-1}, respectively, is shown in Fig. 6(a). Synthetic traveltime data were generated at a wide-angle range from the reflector at 40 km depth. Subsequently, Gaussian noise (mean = 0 and standard deviation = 0.1 s) was added to the synthetic data and then they were plotted (T^2 versus X^2) as shown in Fig. 6(b). A polynomial with an rms error of 0.014 s in T has been fitted (see the inset). The coefficients thus determined were used to evaluate dT/dX using eq. (6) and Z values were computed using eq. (5). The Z values were then plotted against X^2 while the linear regression gives an estimated depth of 41 km at zero-offset as compared with the original depth of 40 km (Fig. 6c). The depth thus obtained is used to calculate the effective velocities at various offsets using eq. (3). The linear regression of the square of the effective velocity versus the square of the offset yields an estimated average velocity of 6.10 km s^{-1} at zero-offset (Fig. 6d), which is close to the actual average velocity of 6.01 km s^{-1}.

We have also studied the effect of velocity variations within the model on the estimated depth of a deeper reflector with increasing offset. The depths have been calculated by segmenting the traveltime data with 20 data points in each segment with increasing offset (as described in Fig. 3). Fig. 7(a) shows the percentage error in depth

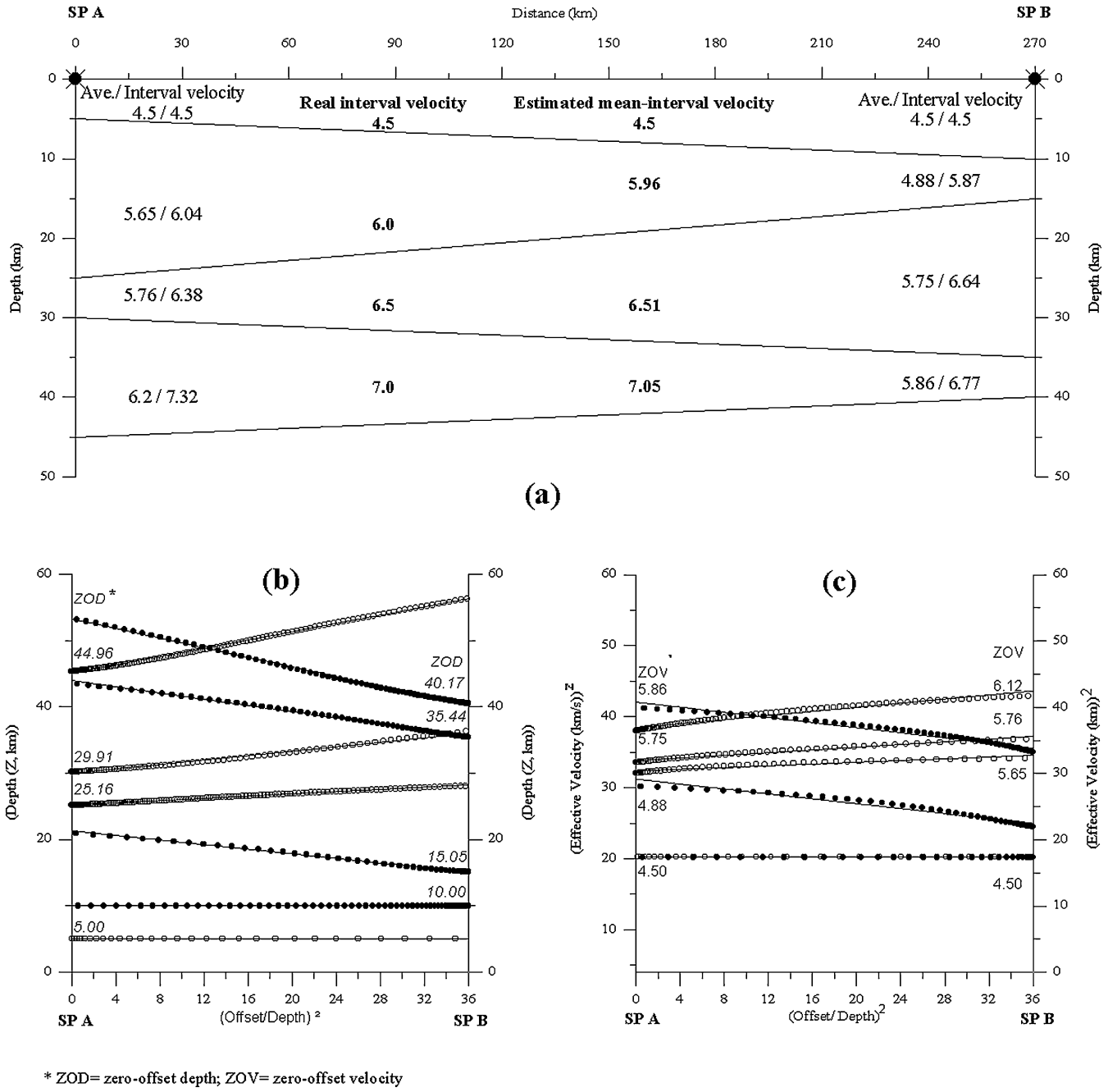

* ZOD= zero-offset depth; ZOV= zero-offset velocity

Figure 5. The slant depths and effective velocities for the traveltime data from two reversed shots (SP A and SP B) were calculated on the basis of a dipping layer model (a) and are plotted in (b) and (c) up to an offset/depth ratio of 6. The average velocities calculated below each shot point are then converted to interval velocities using the corresponding depth values. The arithmetic mean of the interval velocities is the estimated interval velocity of the respective depth interval.

for the 40 km depth reflector of four-layered crustal models that comprise different interval velocities for the individual layers but constant thicknesses, while Fig. 7(b) shows the percentage errors for the same reflector based on models with variable thicknesses of the individual layers but the same velocity structure. It is evident from this study that for the depth estimation of the deep reflector the velocity variations (error ±5 per cent in Fig. 7a) in the overlying layers have more effect than the thickness variations (error ±3 per cent in Fig. 7b).

Finally, we apply the presented method to a field data set that was collected in the western Dharwar craton on the Indian peninsula shield. A crustal velocity structure (Fig. 8) was derived by Sarkar *et al.* (2001) using 2-D forward modelling of the wide-angle reflection data from shotpoints SP 370, 570 and 600. Two sets of traveltime data, one from the mid-crustal level and the other from the Moho level, are displayed in Fig. 8 by different symbols. The data are fitted by a low-order polynomial as mentioned earlier and dT/dX is calculated using eq. (6). Depths and average velocities are then estimated as described in Fig. 2 and are plotted below the shot points (Fig. 8). The estimated depth values are 25.82, 22.78 and 23.73 km for the mid-crustal layer and 40.41, 38.56 and 33.23 km for the Moho, respectively. The arithmetic means of interval

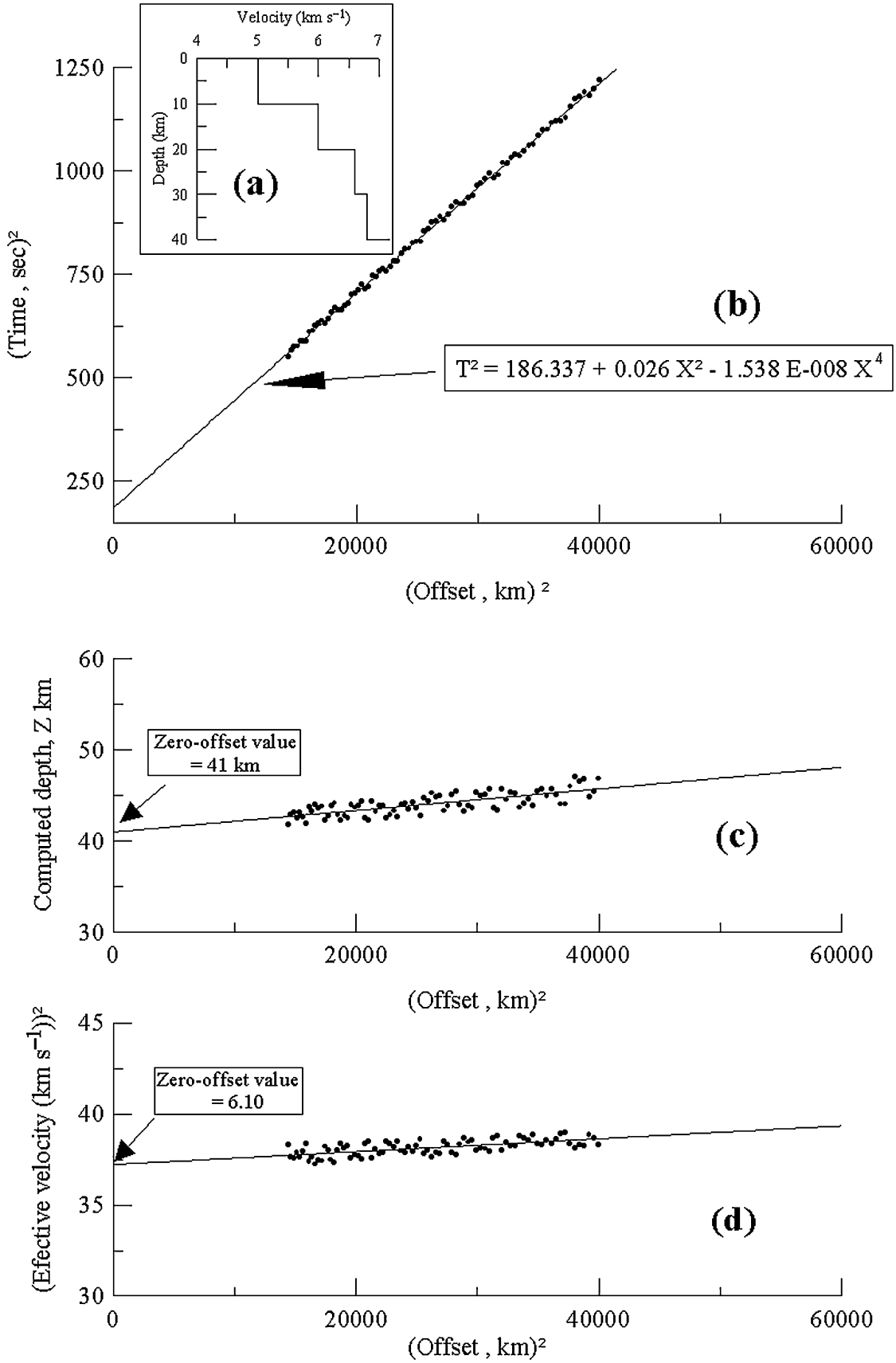

Figure 6. The $T^2 - X^2$ data based on the 1-D velocity model in (a) have been fitted by a polynomial with an rms error of 0.014 s (b). (c) Represents the plot of Z versus X^2 (Z, slant depth; X, offset). The zero-offset Z value obtained by linear regression, is 41 km, which is comparable to the actual depth of 40 km (c). (d) Shows the effective velocity versus X^2. The estimated average velocity (6.10 km s^{-1}) matches quite well with the actual average velocity (6.01 km s^{-1}).

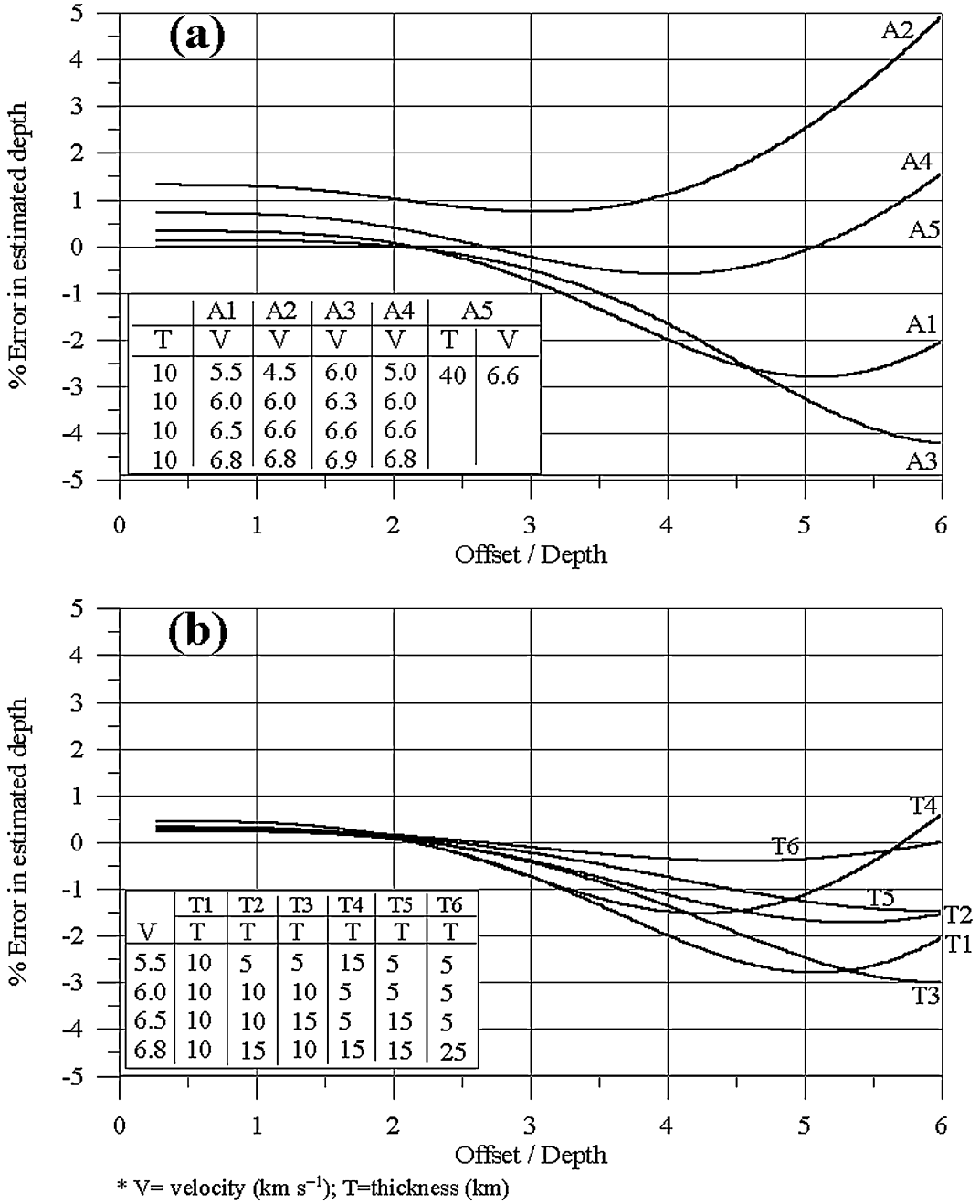

	A1	A2	A3	A4	A5	
T	V	V	V	V	T	V
10	5.5	4.5	6.0	5.0	40	6.6
10	6.0	6.0	6.3	6.0		
10	6.5	6.6	6.6	6.6		
10	6.8	6.8	6.9	6.8		

	T1	T2	T3	T4	T5	T6
V	T	T	T	T	T	T
5.5	10	5	5	15	5	5
6.0	10	10	10	5	5	5
6.5	10	10	15	5	15	5
6.8	10	15	10	15	15	25

Figure 7. (a) Percentage errors in depth for constant thickness and velocity variations of the overlying layers above the reflector at 40 km depth and are plotted against the offset/depth ratio. The errors are within ±5 per cent (i.e. ±2 km). The table shows the different velocity–depth models A1–A4 having four layers with constant thickness of 10 km each and A5 with only a single crustal layer. (b) Percentage error in depth for constant velocities and varying thicknesses of the overlying layers for the reflection from the depth of 40 km and are plotted against the offset/depth. The errors are within ±3 per cent (i.e. ±1.2 km). In both cases, the near-offset errors are small. The table shows the different velocity–depth models T1–T6. While using the constant velocity within the individual layers, their thicknesses were varied.

velocities estimated for the respective layers are 6.13 and 6.73 km s^{-1}. The solutions are in close agreement with the depths and layer velocities calculated by the 2-D forward modelling technique.

4 ADVANTAGES AND LIMITATIONS

(1) Here we presented a very simple method in order to determine the depth to any reflector from any large-offset reflection data.

(2) This method can also be employed to reverse coverage reflection data to estimate the dips of the reflectors provided the dip of the reflector is small ($<10^\circ$). For dips greater than 10°, one has to use the traveltime data beyond an offset/depth ratio of 2.

(3) The effective velocity function for a given model can be determined directly from the traveltime reflection data.

(4) The average velocity above a reflector and hence the interval velocity between two successive reflectors can also be determined from the reflection traveltime data.

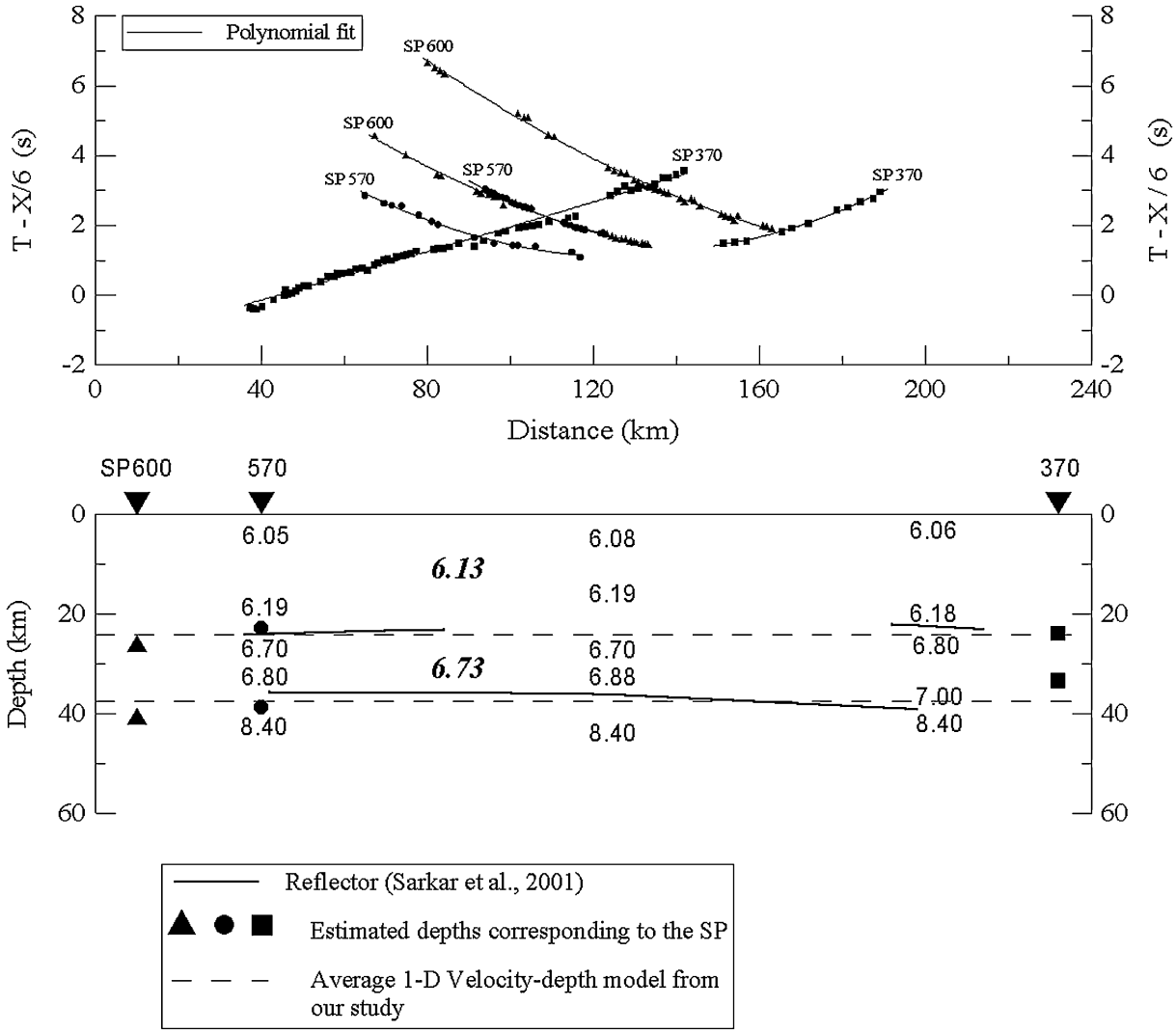

Figure 8. Crustal section through the western Dharwar craton of the Indian peninsula shield. The inverted solid triangles represent the shot point locations (SP600, 570 and 370). The solid lines in the 2-D model represent the reflectors defined by Sarkar *et al.* (2001) based on the ray-tracing method. The estimated depths (▲, ●, ■) derived from the respective reflection traveltimes (shown by corresponding symbols) of three shot points are displayed. The numbers in italics are the estimated mean interval velocities of corresponding individual layers.

(5) The method can be applied to field data, which are not severely disturbed by tectonic activities, and generates an average 1-D velocity model. The traveltime data should not contain large gaps.

ACKNOWLEDGMENTS

The authors thank Dr V. P. Dimri, Director, National Geophysical Research Institute, for his kind permission to publish the paper. We are grateful to Dr Timothy J. Henstock and an anonymous reviewer for their critical reviews and valuable suggestions that helped to improve the manuscript.

REFERENCES

Al-Chalabi, M., 1974. An analysis of stacking, rms, average and interval velocities over a horizontally layered ground, *Geophys. Prospect.,* **22,** 458–475.

de Franco, R., 2001. Interval velocity and thickness estimate from wide-angle reflection data, *Geophys. Prospect.,* **49,** 395–404.

Dix, C.H., 1955. Seismic velocity from surface measurements, *Geophysics,* **20,** 68–86.

Giese, P., 1976. Depth calculation, in *Exploration Seismology in Central Europe,* pp. 156–161, eds Giese, P., Prodhel, C. & Stein, A., Springer, Berlin.

Gonzalez-Serrano, A. & Claerbout, J.F., 1984. Wave-equation velocity analysis, *Geophysics,* **49,** 1432–1456.

Kaila, K.L. & Krishna, V.G., 1979. A new computerized method for finding effective velocity from reversed reflection travel time data, *Geophysics,* **44,** 1064–1076.

Richards, T.C., 1961. Motion of the ground on arrival of reflected longitudinal and traverse waves at wide-angle reflection distance, *Geophysics,* **26,** 277–297.

Robinson, E.A., 1983. *Seismic Velocity Analysis and the Convolutional Model,* D. Reidel Pub. Co., Dordrecht/Boston/Lancaster.

Sain, K. & Kaila, K.L., 1994a. Errors in rms velocity and zero-offset two-way time as determined from wide-angle seismic reflection times using truncated series, *J. Seismic Expl.,* **3,** 173–188.

Sain, K. & Kaila., K.L., 1994b. Inversion of wide-angle seismic reflection times with damped least square, *Geophysics,* **59,** 1735–1744.

Sain, K. & Kaila, K.L., 1996. Direct calculation of interval velocities and layer thicknesses from wide-angle seismic reflection times, *Geophys. J. Int.,* **125,** 30–38.

Sarkar, D., Chanderakala, P., Padmavati Devi, P., Sridhar, A.R., Sain, K. & Reddy, P.R., 2001. Crustal velocity structure of western Dharwar Craton, South India, *J. Geodyn.,* **31,** 227–241.

Schultz, P.S., 1982. A method for direct estimation of interval velocities, *Geophysics,* **47,** 1657–1671.

Slotnick, M.M., 1959. *Lessons in Seismic Computing,* Society of Exploration Geophysicists, Tulsa, OK.

Stoffa, P.L., Bhul, P. & Wenzel, F., 1981. Direct mapping of seismic data to the domain of intercept time and ray parameter—a plane wave decomposition, *Geophysics,* **46,** 255–267.

Winterstein, D.F. & Hanten, J.B., 1985. Super-critical reflections observed in *P*- and *S*-wave data, *Geophysics,* **50,** 185–190.